

## ROTATION ERROR MODELING AND IDENTIFICATION FOR ROBOT KINEMATIC CALIBRATION BY CIRCLE POINT METHOD

Jorge Santolaria<sup>1)</sup>, Javier Conte<sup>1)</sup>, Marcos Pueo<sup>2)</sup>, Carlos Javierre<sup>3)</sup>

1) *Department of Design and Manufacturing Engineering, University of Zaragoza, Zaragoza, Spain. (✉ [jsmazo@unizar.es](mailto:jsmazo@unizar.es) +34976761887).*

2) *Centro Universitario de la Defensa, Zaragoza, Spain.*

3) *Department of Mechanical Engineering, University of Zaragoza, Zaragoza, Spain.*

### Abstract

Screw axis measurement methods obtain a precise identification of the physical reality of the industrial robots' geometry. However, these methods are in a clear disadvantage compared to mathematical optimisation processes for kinematical parameters. That's because mathematical processes obtain kinematical parameters which best reduce the robot errors, despite not necessarily representing the real geometry of the robot. This paper takes the next step at the identification of a robot's movement from the identification of its real kinematical parameters for the later study of every articulation's rotation. We then obtain a combination of real kinematic and dynamic parameters which describe the robot's movement, improving its precision with a physical understanding of the errors.

Keywords: Circle point, Robot calibration, Laser tracker, Mathematical optimization.

© 2014 Polish Academy of Sciences. All rights reserved

### 1. Introduction

The principal objective of robot calibration methods is to increase the robot accuracy [1]. This is translated into obtaining a series of parameters which connect the values of the rotation angle of every robot's axis to the spatial coordinates of the robot's hand (or the mechanism held in it). Determining these parameters can be undertaken with two different procedures. The first corresponds to (open or closed) loop methods, which are based on the measurement of predefined positions of the robot, for the later mathematical optimization of the parameters which better fit the measured positions. The second consists of the screw axis measurement methods, which seek to accurately determine the real positions of the robot's articulation axes, to later obtain the kinematic parameters by means of the algebraic relations existing between the axes [2].

Despite assuming that screw axis measurement methods should provide very precise results as these methods work with the physical reality of the robot, the highest accuracy is obtained by means of the loop methods. This is because the errors produced by the robot's movements are not only due to the geometric errors of its articulations, but are necessary to consider more sources of error. The mathematically optimized parameters artificially include the influence of the other sources of error, therefore obtaining more precise results (despite not being real).

Structural, kinematic and dynamic sources of error [3] can be differentiated from all the sources of error to be analyzed. Structural errors are difficult to predict, as they depend on variables such as the load, temperature, friction, or the robot's wear. This paper studies the other two sources of error: kinematic and dynamic. First, kinematic sources of error will

be studied by calculating the real kinematic parameters of the robot using circle point analysis. Then, dynamic error sources will be studied, analyzing the movement of each articulation independently. Using a Fourier series analysis, the eccentric movement equation is determined for each axis, depending on the displaced angle.

This way, the combination of the kinematic parameters with the eccentric movement parameters provides both a real image of the robot's behavior, and a function which connects with great precision the angle displacements of each articulation to the robot's hand movement.

This new calibration method presents two important advantages. The robot's precision improves when compared to previously used methods, and, the influence of each source of error over the robot's movement can be independently studied.

## 2. Kinematic model of the robot

The mechanism used for the tests is a Kuka robot, model KR 5 sixx R650, whose dimensions are as shown in Fig. 1.

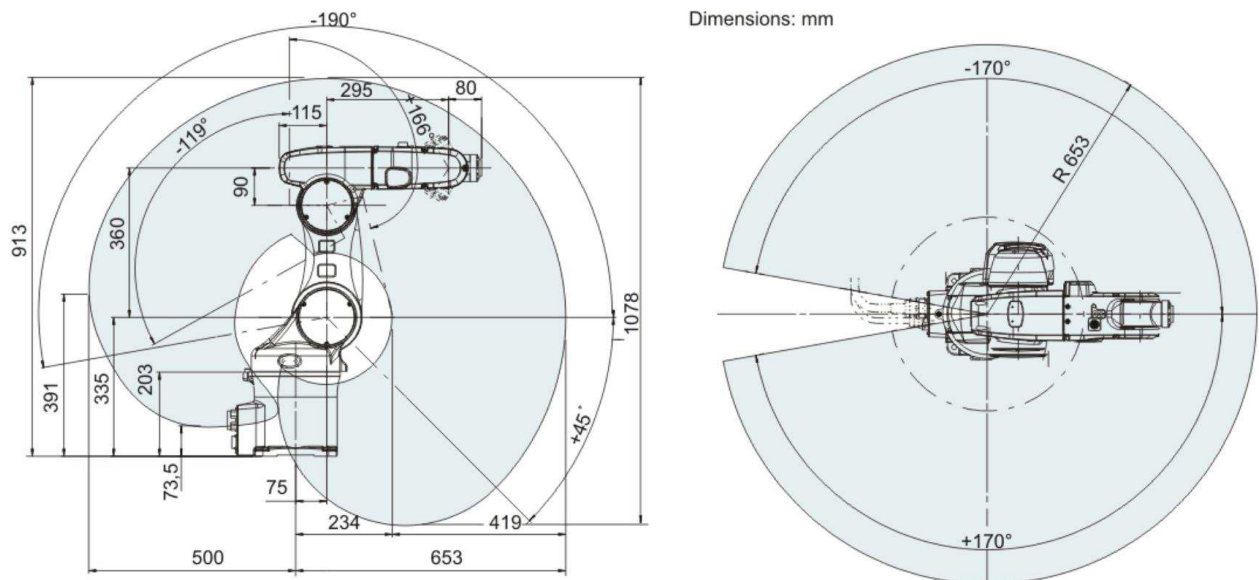


Fig. 1. Robot dimensions.

The first step in calibrating the robot is to define its kinematic model. Due to its simplicity and its generalized use, the four parameter methods defined by Denavit and Hartenberg have been used, plus the particular parameter introduced by Hayati and Mirmirani [4, 5] to overcome the uncertainties produced in the case of almost parallel axes. The value of the said parameters depends on both the robot's dimensions and the coordinate systems defined for every articulation. Fig. 2 shows the defined coordinate systems. According to the proposed method, the robot's kinematic parameters are as shown in Table 1.

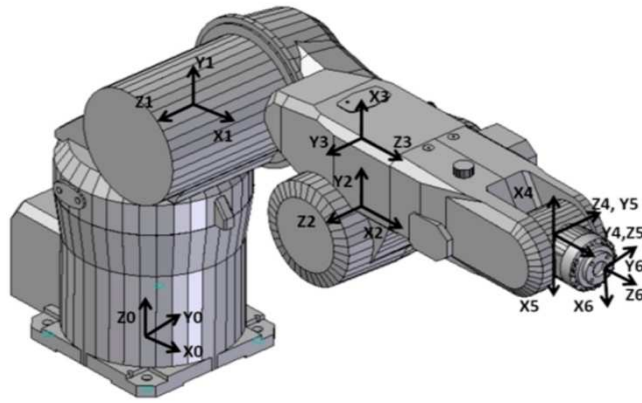


Fig. 2. Robot joint's coordinate systems.

According to the proposed method, the robot's kinematic parameters are as shown in Table 1.

Table 1. Nominal kinematic parameters.

KM PARAM	d (mm)	$\theta$ (°)	a (mm)	$\alpha$ (°)	$\beta$ (°)
Joint 1	335	0	75	90	0
Joint 2	0	0	270	0	0
Joint 3	0	90	90	90	0
Joint 4	295	0	0	90	0
Joint 5	0	180	0	90	0
Joint 6	80	0	0	0	0

Fig. 3 a) and b) shows the kinematic parameters corresponding to the two first pairs of joints.

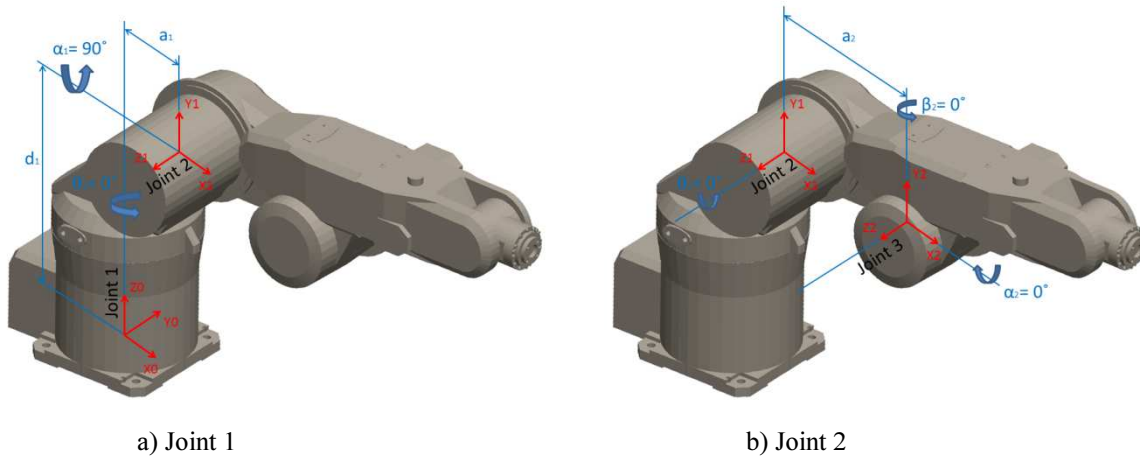


Fig. 3. Kinematic parameters joint 1 and 2.

Once the different reference frames for each joint are established, all the homogeneous transformation matrix that relates coordinates in the  $j$  frame with its corresponding coordinates in the  $j-1$  frame can be calculated. Thus, a point  $r_j$  expressed in the  $j$  frame can be expressed in the  $j-1$  frame as  $r_{j-1}$ , performing two turns and two lineal displacements according to the kinematic parameters of the joint.

Each of these four movements can be expressed by a homogeneous matrix. The product of these four homogeneous transformation matrix results in a homogeneous transformation matrix  ${}^{j-1}A_j$  known as the DH transformation matrix for the  $j$  and  $j-1$  adjacent frames (1).

$${}^{j-1}A_j = T_{z,d}T_{z,\theta}T_{x,a}T_{x,\alpha} = \begin{bmatrix} \cos\theta_j & -\cos\alpha_j\sin\theta_j & \sin\alpha_j\sin\theta_j & a_j\cos\theta_j \\ \sin\theta_j & \cos\alpha_j\cos\theta_j & -\sin\alpha_j\cos\theta_j & a_j\sin\theta_j \\ 0 & \sin\alpha_j & \cos\alpha_j & d_j \\ 0 & 0 & 0 & 1 \end{bmatrix}. \quad (1)$$

Matrix  ${}^0T_j$  specifies the location of the  $j$  frame with respect to the home frame. It is the result of the product of successive transformation matrix  ${}^{j-1}A_j$  and is expressed as (2):

$${}^0T_j = {}^0A_1{}^1A_2\dots{}^{j-1}A_j. \quad (2)$$

The coordinates of a point expressed in the last frame of reference for any position and orientation of the mechanism can be obtained in the home frame (3) following the methodology presented here.

$$\begin{bmatrix} X \\ Y \\ Z \\ 1 \end{bmatrix}_0 = {}^0T_n \begin{bmatrix} X \\ Y \\ Z \\ 1 \end{bmatrix}_n. \quad (3)$$

However, the DH model leads to singularities when two consecutive joints are parallel or nearly parallel. The singularity occurs because small variations between the nominal and real model cause large variations in the DH parameters. This leads to numerical fluctuation when the parameters are identified.

There have been different approaches to solve this problem. The model proposed by Hayati and Mirmirani modifies the DH model by replacing the distance parameter  $d_j$  with an angular parameter  $\beta_j$ . However, this model is only effective for parallel or nearly parallel joints and not for generic representation. The actual model used in this work is a hybrid model with the DH model being used for joints in general and the Mirmirani Hayati model being used for parallel joints. This model will add parameter  $\beta_2$  (4) in the parallel or almost parallel joint angle corresponding to the axes  $Z_2$  and  $Z_3$ . The inclusion of this parameter gives the transformation matrix between adjacent joints (5).

$$T_{y,\beta} = \begin{bmatrix} \cos\beta_j & 0 & \sin\beta_j & 0 \\ 0 & 1 & 0 & 0 \\ -\sin\beta_j & 0 & \cos\beta_j & 0 \\ 0 & 0 & 0 & 1 \end{bmatrix}, \quad (4)$$

$${}^{j-1}A_j = T_{z,d}T_{z,\theta}T_{x,a}T_{x,\alpha}T_{y,\beta}. \quad (5)$$

### 3. Circle Point Method

Circle Point Method [6, 7] is defined by its capacity to determine the spatial positions of rotation axis for any mechanism with rotatory articulations. This is achieved measuring the coordinates of a sensor positioned in the last articulation of the mechanism. This way, the measurements have to correspond to the sensor's circular trajectories, rotating around every mechanism's articulations.

This method is based on the measurement of the position of a sensor rotating around each rotatory joint of the mechanism. Measured trajectories ideally describe a set of perfect circles. The joint axes will be the lines perpendicular to every circle by their center points. Once the position of every axis is calculated, the determination of the robot kinematic parameters can be obtained as the relationships of distances and angles between every two pair of consecutive axes.

The first trajectory to measure corresponds to the rotation of the articulation following to the mechanism's baseplate. From that point on, the following articulations are consecutively measured, following the kinematic chain order. It is fundamental that once measured one articulation, its position does not vary whilst measuring the rest of the articulations so as not to interfere with the process.

The four parameters used to fully specify a single joint are: the length of the joint ( $a$ ), the angle of rotation ( $\alpha$ ), the size of the displacement of the joint ( $d$ ) and the joint angle ( $\theta$ ). Each of these model parameters are defined as follows:

Length articulation  $\vec{a}_{ij}$ : The perpendicular distance between the adjacent axes  $i$  and  $j$ . This is the magnitude of vector mutually perpendicular joint.

Rotation angle  $\vec{a}_{ij}$ : The angle between adjacent axes  $i$ ,  $j$ , and measured as the clockwise rotation from  $\vec{S}_i$  to  $\vec{S}_j$  around vector  $\vec{a}_{ij}$ . The following definition ensures this restriction directional (6), (7):

$$\cos \alpha_j = c_{ij} = \vec{S}_i \times \vec{S}_j, \quad (6)$$

$$\sin \alpha_{ij} = s_{ij} = (\vec{S}_i \times \vec{S}_j) \cdot \vec{a}_{ij}. \quad (7)$$

Displacement  $d_j$ : the displacement distance between two joints given as the distance between  $\vec{a}_{ij}$  and  $\vec{a}_{jk}$  along the axis  $\vec{S}_j$ .

Joint angle  $\theta_j$ : This is the kinematic parameters defining the relationship between adjacent joints. The angle between adjacent joints  $ij$  and  $jk$ , and is measured as a clockwise rotation from vector  $\vec{a}_{ij}$  to  $\vec{a}_{jk}$  around  $\vec{S}_j$ . The following definition ensures this restriction directional (8), (9):

$$\cos \theta_j = c_j = \vec{a}_{ij} \times \vec{a}_{jk}, \quad (8)$$

$$\sin \theta_j = s_j = (\vec{a}_{ij} \times \vec{a}_{jk}) \cdot \vec{S}_j. \quad (9)$$

A graphical description of preceding formulae is shown on Fig. 4.

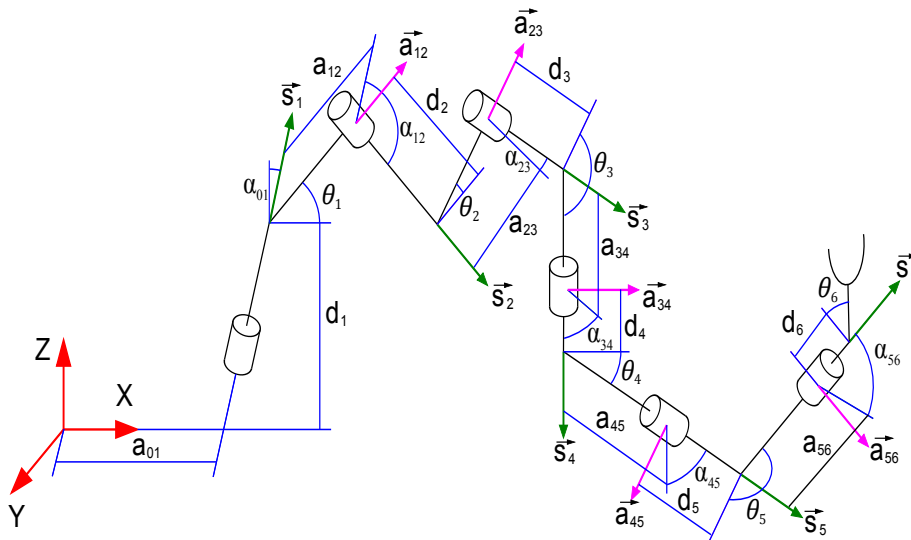


Fig. 4. Description of a 6-degrees of freedom manipulator.

In an ideal situation, the mechanism's kinematic model allows the coordinates of the final effector in relation to the origin reference system of the mechanism to be known, depending on the articulation's angle displacements.

In reality, there are errors which provoke the existence of differences between the theoretical positions of the mechanism's rotation axis and its real position. In this situation the circle point method helps in finding the mechanism's real geometry and correcting its kinematic model with the measured positions of its rotation axis.

This method requires a sensor, capable of moving, to be joined to every articulation, and a coordinate measurement system, which provides the coordinates of the said sensor along its trajectory. The laser tracker (LT) has been widely used for this kind of measurement due to its accuracy and ease in following the displacement of optical reflectors adhered to the mechanism's articulations [8, 9]. These static reflectors present two important problems. On the one hand, the measuring precision depends on the laser's angle of incidence on the reflector, this is why, as the reflector keeps on spinning, the measurements' precision decreases: On the other, the aforementioned angle of incidence is limited, which makes it impossible to measure more than one part of the articulation's rotation, thus making it necessary to measure parts by reorientating the articulation as the line of vision with the LT is lost. This introduces a measuring error factor due to the sensor's repositioning uncertainty.

The realized study used an active tracking sensor, designed by the API brand which assembles an optical reflector, with two degrees of freedom, within a tracking mechanism, similar to the LT head. This mechanism searches the laser's direction in the same way as the LT follows the reflector. This provides a permanent line of vision between the LT and the reflector, which allows the measurements to be realized by a continuous process, and with an adequate angle of incidence on the reflector.

#### 4. Experimental setup

The following elements were used to develop the calibration process:

KUKA Robot KR5 sixx. This is the mechanism to be calibrated. It is a small six axis robot with a reach of 650 mm and a 5 kg payload. The repeatability is  $\pm 0.02$  mm according to ISO 9283 but it's accuracy is only 0,5 mm according to previous tests.

API laser tracker 3. This is a high range measurement device with a range of 15 m and accuracy of  $\pm 15$   $\mu\text{m}$  or 1.5 ppm. with ADM. We have placed the LT as near as possible to the robot and we are working on a range of 2,5 m from the LT, so our accuracy is  $\pm 3,75$   $\mu\text{m}$ . This measuring device is connected to a commercial software to capture the points data.

Active target API. This is a spherical reflector (SMR) mounted on a 2 DOF mechanism. The reflector of the Active Target works similarly to any standard SMR. The difference is that the Active Target features built-in technology motorisation that automatically positions the reflector to face the tracker. Its optical accuracy is  $\pm 3$   $\mu\text{m}$ . Fig. 5 shows the experimental setup described.

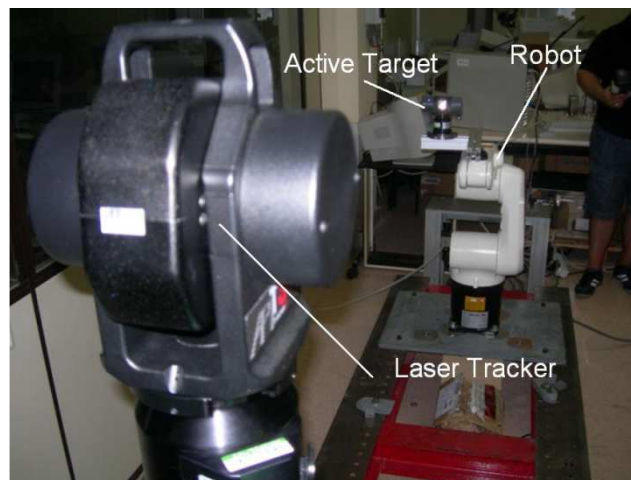


Fig. 5. Experimental setup.

A specific software has been developed to capture the data of the robot. Through an interface between the robot and an external computer, the angles of the robot at each predetermined position can be captured. These data, along with the Active Target positions obtained by the LT, are analysed to give the information required to calibrate the robot.

To program the movements of the robot, an automatic generator has also been developed. Using variables such as the initial and final positions of each axis, the number of captured points and the number of runs, the program generates the robot program which commands the robot and controls the communication between the robot and the external data capture device.

## 5. Tests and results

Different tests were undertaken varying the points' sample size, the range of movement of every articulation and their rotating speeds. Table 2 gathers the main characteristics of every test.

Table 2. Measured angles by test

		Test 1	Test 2	Test 3	Test 4	Test 5	Test 6
Joint 1	Start	167°	167°	167°	80°	80°	80°
	End	-167°	-167°	-167°	-80°	-80°	-80°
	Range	334°	334°	334°	160°	160°	160°
	Points	10	60	30	30	30	30
	Angle step	33,40°	5,57°	11,13°	5,33°	5,33°	5,33°
Joint 2	Start	-5°	-5°	-5°	-40°	-40°	-40°
	End	-162°	-162°	-162°	-120°	-120°	-120°
	Range	157°	157°	157°	80°	80°	80°
	Points	10	30	15	15	15	15
	Angle step	15,70°	5,23°	10,47°	5,33°	5,33°	5,33°
Joint 3	Start	145°	145°	145°	80°	80°	80°
	End	-114°	-114°	-114°	-50°	-50°	-50°
	Range	259°	259°	259°	130°	130°	130°
	Points	10	50	25	25	25	25
	Angle step	25,90°	5,18°	10,36°	5,20°	5,20°	5,20°
Joint 4	Start	177°	177°	177°	90°	90°	90°
	End	-177°	-177°	-177°	-90°	-90°	-90°
	Range	354°	354°	354°	180°	180°	180°
	Points	10	60	30	30	30	30
	Angle step	35,40°	5,90°	11,80°	6,00°	6,00°	6,00°
Joint 5	Start	90°	90°	90°	45°	45°	45°
	End	-90°	-90°	-90°	-45°	-45°	-45°
	Range	180°	180°	180°	90°	90°	90°
	Points	10	30	15	15	15	15
	Angle step	18,00°	6,00°	12°	6,00°	6,00°	6,00°
Joint 6	Start	178°	178°	178°	90°	90°	90°
	End	-178°	-178°	-178°	-90°	-90°	-90°
	Range	356°	356°	356°	180°	180°	180°
	Points	10	60	30	30	30	30
	Angle step	35,60°	5,93°	11,87°	6,00°	6,00°	6,00°
% of max robot speed		3%	3%	3%	1%	3%	10%
Measured points		120	580	290	290	290	290

Once the sensor’s trajectories have been measured, the circle point method can be used. Each circular trajectory is independently dealt with, following this procedure:

1. Calculate the best-fitting plane for every trajectory using the method of least squares.
2. Project the captured points onto the plane.
3. With the calculated points, obtain the best-fitting circumference (to said points), using least squares method.
4. The circumference’s center will be a point in the rotation axis of the articulation.
5. The rotation axis’ direction will be perpendicular to the plane which contains the circle.

Once the spatial positions of the articulations’ rotation axes are obtained, linear algebra [7] can be used to calculate the distances and angles between consecutive axes, which correspond to the robot’s kinematic parameters.

The parameters calculated following this method are as show in Table 3:



Table 3. Circle Point kinematic parameters

	Nom.	Test 1	Test 2	Test 3	Test 4	Test 5	Test 6	Avg. 1-6	$\sigma$ 1-6	Avg. 2-6	$\sigma$ 2-6
d1 (mm)	335	332,8307	335,2766	335,3591	335,1712	335,1850	335,2024	334,8375	0,9856	335,2389	0,0786
d3 (mm)	0	-0,5332	-0,3389	-0,3440	-0,3455	-0,3495	-0,3506	-0,3769	0,0767	-0,3457	0,0047
d4 (mm)	295	294,2804	295,2578	295,2325	295,2997	295,2996	295,2997	295,1116	0,4082	295,2779	0,0312
d5 (mm)	0	0,1751	0,0290	0,0271	-0,0092	-0,0082	-0,0071	0,0345	0,0712	0,0063	0,0199
$\theta 1$ (°)	0	0,1267	0,0778	0,0971	0,0745	0,0754	0,0766	0,0880	0,0208	0,0803	0,0095
$\theta 2$ (°)	0	-0,1459	-0,0236	-0,0225	-0,0344	-0,0332	-0,0301	-0,0483	0,0481	-0,0288	0,0055
$\theta 3$ (°)	90	90,1702	89,9429	89,9436	89,9552	89,9525	89,9498	89,9857	0,0905	89,9488	0,0054
$\theta 4$ (°)	0	0,2016	0,2071	0,2095	0,2151	0,2150	0,2147	0,2105	0,0055	0,2123	0,0037
$\theta 5$ (°)	180	180,0416	180,0626	180,0611	180,0604	180,0609	180,0605	180,0579	0,0080	180,0611	0,0009
a1 (mm)	75	74,7028	74,8693	74,8659	74,8040	74,8200	74,8241	74,8144	0,0606	74,8367	0,0292
a2 (mm)	270	271,6223	270,3284	270,3301	270,3621	270,3476	270,3344	270,5542	0,5234	270,3405	0,0142
a3 (mm)	90	89,8065	90,2592	90,2418	90,2867	90,2930	90,2970	90,1974	0,1927	90,2756	0,0239
a4 (mm)	0	-0,2582	-0,0371	-0,0378	-0,0262	-0,0316	-0,0263	-0,0695	0,0926	-0,0318	0,0056
a5 (mm)	0	0,5201	0,0114	0,0145	-0,0103	-0,0106	-0,0065	0,0864	0,2127	-0,0003	0,0122
$\alpha 1$ (°)	90	90,0208	90,0173	90,0161	90,0166	90,0178	90,0175	90,0177	0,0016	90,0171	0,0007
$\alpha 2$ (°)	0	0,0063	0,0051	0,0057	0,0089	0,0096	0,0090	0,0074	0,0020	0,0077	0,0021
$\alpha 3$ (°)	90	89,9701	89,9701	89,9698	89,9704	89,9703	89,9703	89,9702	0,0002	89,9702	0,0002
$\alpha 4$ (°)	90	90,0366	90,0269	90,0263	90,0301	90,0304	90,0313	90,0303	0,0037	90,0290	0,0022
$\alpha 5$ (°)	90	90,0298	90,0160	90,0153	90,0194	90,0199	90,0203	90,0201	0,0052	90,0182	0,0023
$\beta 2$ (°)	0	0,0533	0,0509	0,0531	0,0554	0,0565	0,0547	0,0540	0,0020	0,0541	0,0022

Once the robot's kinematic parameters for each test are obtained, it is necessary to define a criterion which allows us to check if we have succeeded in improving the robot's precision, and to what extent.

The chosen criterion is based on the calculation of the relative distances between every pair of points of the sample. The optimum value will be obtained from the calculation of the distances between the points measured using the LT. From each one of these distances is subtracted the distances between those same points, referred to as the robot's reference system, first calculated with the nominal parameters and then with the parameters obtained using the circle point method. By doing this we will obtain two vectors of  $N \times (N-1)/2$  elements ( $N$  being the sample size), having in the first vector the differences between the points measured with the LT and those obtained with the nominal parameters. The second vector contains the differences between the points measured with the LT and those obtained with the circle point parameters.

Analyzing the maximum and average values of the said vectors, it is determined which of the two sets of parameters provides the highest accuracy and to what extent.

The results of the tests regarding the precision improvement obtained with the kinematic parameters calculated with regard to the nominal parameters are shown in Table 4.

Table 4. Error comparison between nominal and Circle Point parameters.

	Nominal parameters		Circle Point parameters		Improvement
	Average error (mm)	Maximum error (mm)	Average error (mm)	Maximum error (mm)	
Test 1	1,3444	4,8369	1,5587	4,0045	-13,75%
Test 2	0,4619	1,7168	0,4031	1,4906	14,59%
Test 3	0,4883	1,7035	0,4152	1,4652	17,61%
Test 4	0,4363	1,5403	0,2901	1,3057	50,40%
Test 5	0,4406	1,5653	0,2946	1,3151	49,56%
Test 6	0,4399	1,5716	0,2907	1,3083	51,32%

It is verified that the first test must be discarded due to the reduced size of the sample. Regarding the rest of the tests, it can be perceived that the better defined the robot's work area (Tests 4 to 6), the more precise are the optimizations. It is logical that it is more difficult to obtain a general calibration than a local one.

We can deduce that, always discarding the first test and given that the deviations are very low, important variations with regard to the obtained kinematic parameters cannot be perceived. This is why, so long as a sample with enough points can be found, the influence of the robot's velocity or the influence due to the increase in the sample size do not pose important variations for the calculated kinematic parameters. This situation would be different in the event of using low angular paths, a case in which it would be possible to obtain unreliable results.

It can be verified that the backlash error is very high in several articulations, fundamentally in the four reaching values of 250  $\mu\text{m}$ , which makes it impossible to reach the robot's nominal values of repeatability of  $\pm 20\mu\text{m}$ . This highly conditions the method's accuracy given that it is not possible to find parameters which eliminate this error, as it depends on every movement of the robot's axes directions, and it is not easy to systemize the way in which the robot is going to move.

### 6. Eccentricity movement analysis

The correction of the kinematic parameters of the robot is not enough to improve the robot accuracy because it is a static correction and the real errors depend also on the position of every joint.

The rotating body shown in Fig. 6 is considered. Ideally, this body rotates over its rotation axis with no error. However, in reality the rotation axis rotates over an axis in the frame of the reference coordinates with radial errors  $\delta_x$  and  $\delta_y$ , an axial error  $\delta_z$ , and sway errors of the axis, called  $\epsilon_x$  and  $\epsilon_y$  [10]. These errors can also depend on the rotation angle  $\theta_z$ . For a point in the frame of the axis, coordinates  $X_n Y_n Z_n$ , its position error can be calculated, depending on the rotation's eccentricity errors, as the product of the error matrixes corresponding to each one of the considered errors.

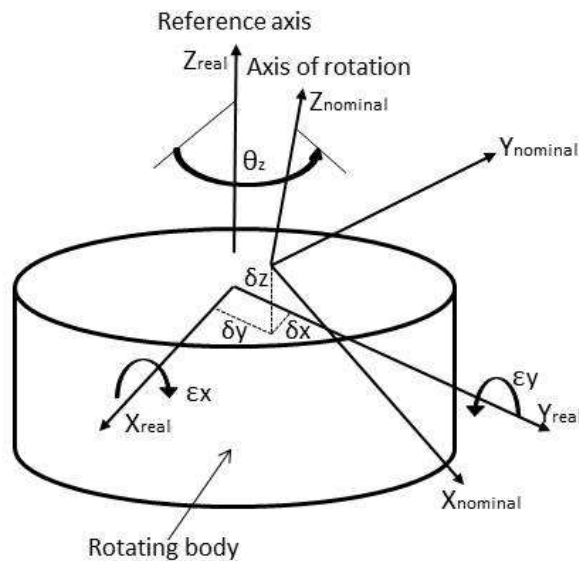


Fig. 6. Produced errors in the movement of rotation axis.

As the other movement errors are small, the homogeneous transformation matrix multiplication order is not critical. The sequenced multiplication of the homogeneous transformation matrixes, which provides the resulting error matrix  $RT_{err}$ , would therefore have the expression (10).

$$RT_{err} = MT_x \cdot MT_y \cdot MT_z \cdot MG_{\theta_x} \cdot MG_{\theta_y} \cdot MG_{\theta_z}, \tag{10}$$

where:

$MT_n$  is the translation matrix of a quantity “n” along the axis “n”, for n=x, y, or z

$MG_{\theta n}$  is the rotation matrix for an angle around the axis “n”, for n=x, y, or z.

The general result after expanding the matrix in the previous equation would be as (11).

$$RT_{err} = \begin{bmatrix} \cos \varepsilon_y \cos \theta_z & -\cos \varepsilon_y \sin \theta_z & \sin \varepsilon_y & \delta_x \\ \cos \varepsilon_x \sin \theta_z + \sin \varepsilon_x \sin \varepsilon_y \cos \theta_z & \cos \varepsilon_x \cos \theta_z - \sin \varepsilon_x \sin \varepsilon_y \sin \theta_z & -\sin \varepsilon_x \cos \varepsilon_y & \delta_y \\ \sin \varepsilon_x \sin \theta_z - \cos \varepsilon_x \sin \varepsilon_y \cos \theta_z & \sin \varepsilon_x \cos \theta_z + \cos \varepsilon_x \sin \varepsilon_y \sin \theta_z & \cos \varepsilon_x \cos \varepsilon_y & \delta_z \\ 0 & 0 & 0 & 1 \end{bmatrix}. \tag{11}$$

The circle point method provides very important information about the robot’s geometry, as it accurately calculates the positions of the rotation axis for each one of its six articulations. This provides an important improvement in its accuracy as it allows us to adjust its parameters to the robot’s physical reality.

In order to obtain a correct calibration of the robot, we need to know the errors the robot makes when rotating around each one of its axes. The circle point method considers the ideal situation in which every axis rotation is perfect and the reflector describes a circle around its rotation axis; this means the reflector acts as an eccentricity.

In reality, any rotation movement around the Z axis will contain five errors, three position errors for each axis,  $d_x$ ,  $d_y$ ,  $d_z$  and two rotation errors,  $\varepsilon_x$ ,  $\varepsilon_y$ .

In order to understand and systemize these errors it is necessary to confer on them a particular expression for analysis.

These errors have been proved to follow a periodic expression with a period of  $2\pi$  radians so they correspond to Fourier series. Several calculations have been made to find out the number of terms necessary from the Fourier series and the improvement obtained from the first term to the following ones is not significant, so we can formulate the rotation errors as shown on (12).

$$Error = D + A \cdot \sin\left(\frac{2\pi}{T} \cdot \theta_z + \varphi\right). \tag{12}$$

The expressions of the errors corresponding to each articulation are as seen on (13) to (17).

$$dx = Ddx + Adx \cdot \sin\left(\frac{2\pi}{Tdx} \cdot \theta_z + \varphi dx\right), \tag{13}$$

$$dy = Ddy + Ady \cdot \sin\left(\frac{2\pi}{Tdy} \cdot \theta_z + \varphi dy\right), \tag{14}$$

$$dz = Ddz + Adz \cdot \sin\left(\frac{2\pi}{Tdz} \cdot \theta_z + \varphi dz\right), \tag{15}$$

$$\varepsilon_x = D\varepsilon_x + A\varepsilon_x \cdot \sin\left(\frac{2\pi}{T\varepsilon_x} \cdot \theta_z + \varphi \varepsilon_x\right), \tag{16}$$

$$\varepsilon_y = D\varepsilon_y + A\varepsilon_y \cdot \sin\left(\frac{2\pi}{T\varepsilon_y} \cdot \theta_z + \varphi \varepsilon_y\right). \tag{17}$$

Once the error expressions have been defined, it is necessary to establish an optimization criterion so as to find the best-fitting parameters for the error expressions. This study utilizes non-linear optimization with least squares by means of the Levenberg–Marquardt algorithm [11]. This algorithm has shown good results in robot and articulated arm coordinate measuring machines calibration techniques [12].

We introduce to this optimization a vector “X” with the parameters to modify and a criterion to check if the modified parameters are better or worse than the originals.

The vector “X” is composed of all the error parameters described in Equations 4 to 8 for each axis. We have three error parameters (D, A and  $\phi$ ) for every error, plus five errors per joint ( $\delta x$ ,  $\delta y$ ,  $\delta z$ ,  $\epsilon x$  and  $\epsilon y$ ) plus six joints so we need  $3 \times 5 \times 6 = 90$  error parameters. The notation Ddx1 means parameter D for error  $\delta x$  in axis 1.

$X = (Ddx1, Ddy1, Ddz1, D\epsilon x1, D\epsilon y1, Adx1, Ady1, Adz1, A\epsilon x1, A\epsilon y1, \phi dx1, \phi dy2, \phi dz1, \phi \epsilon x1, \phi \epsilon y1, \dots, Ddx6, Ddy6, Ddz6, D\epsilon x6, D\epsilon y6, Adx6, Ady6, Adz6, A\epsilon x6, A\epsilon y6, \phi dx6, \phi dy6, \phi dz6, \phi \epsilon x6, \phi \epsilon y6)$

The chosen improvement criterion corresponds to the difference in the distances between the points captured with the LT, considered as the goal distances, and the distances calculated based on the robot’s kinematic parameters obtained with the circle point method and the error matrixes calculated from the parameters “X”. The optimization procedure uses a Matlab function which solves nonlinear least-squares problems. This function automatically varies the parameter values, included in the vector “X”, seeking the least possible difference between the two matrixes. The optimisation criterion formulation can be represented as (18).

$$F = \sum_{i=1}^{n-1} \sum_{j=i+1}^n \left( \left| \vec{u}_{ij}^{LT} \right| - \left| \vec{u}_{ij}^{CP} \right| \right)^2, \quad (18)$$

where:

$F$  is the function to be minimized.

$n$  is the number of captured points

$\left| \vec{u}_{ij}^{LT} \right|$  is the modulus of vector from point  $i$  to point  $j$  in coordinates measured by the Laser Tracker. (LT) or nominal from Circle Point method (CP).

$\left| \vec{u}_{ij}^{CP} \right|$  is the modulus of vector from point  $i$  to point  $j$  according to kinematic parameters calculated with Circle Point method and the rotation error parameters.

The improvement criterion used has the following disadvantage: it can provoke a displacement of the cloud of captured points when varying its parameters. To avoid these displacements, a series of fixed points is included in the calculation; these fixed points are not affected by the error matrixes. The chosen fixed points are the centers of the circles 1, 3, and 5 calculated with the circle point method. These points are added to the list of captured points by the LT in its three first positions and also, and in the same way, to the list of points we calculated in the robot’s reference system. Three points are required because it is the minimum quantity in order to fix the others; if we use only one, the others can rotate around it with two degrees of freedom; and if two are used, the cloud of points can rotate around the line which connects the two points without varying the distance from them.

## 7. Optimisation results

The optimisation has been made only for test 2 because it’s the most general situation, with the largest angular range obtained and the highest amount of data captured.

The obtained parameters are as shown in tables 5 to 7:

Table 5. Eccentricity displacement parameters

	Ddx (mm)	Ddy (mm)	Ddz (mm)	Dex (mm)	Dey (mm)
Joint 1	-0,00894432	-0,00044766	-0,09097568	-2,8886E-05	9,9299E-05
Joint 2	0,00225915	-0,05434195	-0,00171799	-0,00027847	0,00043006
Joint 3	0,16801637	0,00185002	-0,03888246	-0,00021782	-0,0004381
Joint 4	0,00982289	0,03792663	0,00545861	9,5836E-05	-0,00014458
Joint 5	-0,00465192	0,00250222	0,31343338	0,00324521	-0,00115391
Joint 6	-0,03546433	-0,02386418	-0,13111638	0,00084781	0,00031983

Table 6. Eccentricity amplitude parameters

	Adx (mm)	Ady (mm)	Adz (mm)	Aex (mm)	Aey (mm)
Joint 1	-0,09438893	-0,010266	-0,1214897	-0,0056238	0,0062345
Joint 2	-0,01861644	-0,11436569	-0,00977474	0,02706514	-0,02377566
Joint 3	0,14699369	-0,02192545	-0,00973498	0,00430838	0,02144104
Joint 4	0,24364125	-0,00971577	-0,02075261	-0,01180938	0,00267801
Joint 5	-0,1641385	-0,02075231	0,0408056	-0,00131996	-0,14413296
Joint 6	0,00374365	0,04081512	0,02455266	0,01901011	0,04791811

Table 7. Eccentricity phase difference parameters

	$\phi_{dx}$ (rad)	$\phi_{dy}$ (rad)	$\phi_{dz}$ (rad)	$\phi_{ex}$ (rad)	$\phi_{ey}$ (rad)
Joint 1	3,4892E-05	5,8111E-06	0	0	2,3934E-05
Joint 2	0,00017001	2,8559E-05	2,3993E-05	1,7867E-05	1,827E-07
Joint 3	0	0,00026735	0	1,535E-07	2,1815E-05
Joint 4	0	0	0	1,729E-07	1,6947E-05
Joint 5	3,3104E-05	0	5,7802E-05	0	0,00031557
Joint 6	0,00015193	3,6924E-05	1,49E-07	2,7434E-05	0

The obtained quality parameters with this optimization are as follows:

- Average error of the distances between the points: 0.1095735  $\mu\text{m}$
- Maximum error of the distances between the points: 0.8673400  $\mu\text{m}$

## 8. Conclusions

The non-linear optimization results can be considered as very satisfying, as they reduce the average error made with the circle point method from 0.4031 mm to 0.1096 mm, which means to a quarter.

In addition, the obtained parameters are, in total, very low, which represents movement errors compatible with reality.

As expected, the highest parameters are found in the articulations which present greater backlash, as the optimization tries to locate the best-fitting trajectory for those points, which have very different coordinates for the same robot position.

Circle point analysis offers an interesting point of view of robot calibration, but it lacks accuracy. That is because circle point analysis only shows positioning errors of robot axes

and, as seen in this paper, rotatory errors can be a higher source of errors than kinematic parameters.

Despite this, we cannot underestimate the benefits of circle point as a first step in the calibration of a robot's arms. Circle point gives us the real position of the robot's joints which, in conjunction with the study of the dynamic behavior of them, offers full knowledge of the robot's errors under defined conditions of the temperature and the load of the robot's arm.

Usual calibration procedures are based on the determination of the robot's kinematic parameters from a set of measures and a mathematical optimization of the parameters. These procedures give better accuracy than circle point but calculated kinematic parameters are not real, they are just a set of numerical values which best fit with the robot's error.

Circle Point method improved with eccentricity errors can be a more powerful method to calibrate rotatory mechanisms. In this paper a first order eccentricity formulation has been considered but including the study of further harmonics the precision of the calibration can be highly increased.

## References

- [1] Roth, Z.S., Mooring, B.W., Ravani, B (1987). An overview of robot calibration. *IEEE Journal of Robotics and Automation*, 3(5), 377–385.
- [2] Hollerbach, J.M., Wampler, C.W. (1996). The calibration index and taxonomy for robot kinematic calibration methods. *International Journal of Robotics Research*, 15(6),573–591.
- [3] Shiakolas, P.S., Conrad, K.L., Yih, T.C. (2002). On the accuracy, repeatability, and degree of influence of kinematics parameters for industrial robots. *International Journal of Modelling and Simulation*, 22(3), 1–10.
- [4] Denavit, J., Hartenberg, R.S. (1955). A kinematic notation for lower-pair mechanisms based on matrices *Journal of Applied Mechanics*, 77, 215–21.
- [5] Hayati, S.A., Mirmirani, M. (1985). Improving the absolute positioning accuracy of robot manipulators. *Journal of Robotics Systems*, 2, 397–413.
- [6] Stone, H.W. (1987). *Kinematic modeling, identification, and control of robotic manipulators*, Boston: Kluwer Academic Publishers.
- [7] Sklar, M.E. (1989). Geometric calibration of industrial manipulators by circle point analysis. *Proceedings of the 2nd Conference on Recent Advances in Robotics*, 178–202.
- [8] Alici, G., Shirinzadeh, B. (2005). A systematic technique to estimate positioning errors for robot accuracy improvement using laser interferometry based sensing. *Mechanism and Machine Theory*, 40, 879–906.
- [9] Newman, W.S., Birkhimer, C.E., Horning, R.J. (2000) Calibration of a Motoman P8 robot based on laser tracking. *Proceedings of the 2000 IEEE International Conference of Robotics & Automation*, San Francisco, CA, 3597–3602.
- [10] Slocum, A.H. (1992). *Precision machine design*. Society of manufacturing engineers, 61–72.
- [11] Moré, J.J. (1977). *The Levenberg-Marquardt algorithm: Implementation and theory*, in Numerical Analysis, G. A. Watson, ed., Lecture Notes in Mathematics 630, Berlin: Springer-Verlag, 105–116.
- [12] Santolaria, J., Aguilar, J.J., Yagüe, J.A., Pastor, J. (2008). Kinematic parameter estimation technique for calibration and repeatability improvement of articulated arm coordinate measuring machines. *Precision Engineering*, 32, 251–268.